

Article

Fe₃O₄ Nanoparticles in Combination with 5-FU Exert Antitumor Effects Superior to Those of the Active Drug in a Colon Cancer Cell Model

Sidika Genc¹, Ali Taghizadehghalehjoughi^{1,*}, Yesim Yeni², Abbas Jafarizad³, Ahmet Hacimuftuoglu², Dragana Nikitovic⁴, Anca Oana Docea^{5,*}, Yaroslav Mezhuev⁶ and Aristidis Tsatsakis⁷

¹ Department of Medical Pharmacology, Faculty of Medicine, Bilecik Seyh Edebali University, Bilecik 11230, Turkey; sidika.genc@bilecik.edu.tr

² Department of Pharmacology, Faculty of Medicine, Ataturk University, Erzurum 25240, Turkey; yesimyeni.75@outlook.com.tr (Y.Y.); ahmeth@atauni.edu.tr (A.H.)

³ Faculty of Chemical Engineering, Sahand University of Technology, Tabriz 51335-1996, Iran; jafarizad.abbas@gmail.com

⁴ Laboratory of Histology-Embryology, Medical School, University of Crete, 71003 Heraklion, Greece; nikitovic@uoc.gr

⁵ Department of Toxicology, University of Medicine and Pharmacy of Craiova, 200349 Craiova, Romania

⁶ Center of Biomaterials, D. Mendeleev University of Chemical Technology of Russia, 125047 Moscow, Russia; yaroslav.mezhuev@gmail.com

⁷ Department of Forensic Sciences and Toxicology, Faculty of Medicine, University of Crete, 71003 Heraklion, Greece; aristsatsakis@gmail.com

* Correspondence: ali.tgzd@bilecik.edu.tr (A.T.); daoana00@gmail.com (A.O.D.)

Abstract: (1) Background: Colon cancer is one of the most common cancer types, and treatment options, unfortunately, do not continually improve the survival rate of patients. With the unprecedented development of nanotechnologies, nanomedicine has become a significant direction in cancer research. Indeed, chemotherapeutics with nanoparticles (NPs) in cancer treatment is an outstanding new treatment principle. (2) Methods: Fe₃O₄ NPs were synthesized and characterized. Caco-2 colon cancer cells were treated during two different periods (24 and 72 h) with Fe₃O₄ NPs (6 µg/mL), various concentrations of 5-FU (4–16 µg/mL), and Fe₃O₄ NPs in combination with 5-FU (4–16 µg/mL) (Fe₃O₄ NPs + 5-FU). (3) Results: The MTT assay showed that treating the cells with Fe₃O₄ NPs + 5-FU at 16 µg/mL for 24 or 72 h decreased cell viability and increased their LDH release ($p < 0.05$ and $p < 0.01$, respectively). Furthermore, at the same treatment concentrations, total antioxidant capacity (TAC) was decreased ($p < 0.05$ and $p < 0.01$, respectively), and total oxidant status (TOS) increased ($p < 0.05$ and $p < 0.01$, respectively). Moreover, after treatment with Fe₃O₄-NPs + 5-FU, the IL-10 gene was downregulated and PTEN gene expression was upregulated ($p < 0.05$ and $p < 0.01$, respectively) compared with those of the control. (4) Conclusions: Fe₃O₄ NPs exert a synergistic cytotoxic effect with 5-FU on Caco-2 cells at concentrations below the active drug threshold levels.

Keywords: Fe₃O₄ nanoparticles; 5-fluorouracil; Caco-2; PTEN; IL-10; oxidative status



Citation: Genc, S.;

Taghizadehghalehjoughi, A.; Yeni, Y.; Jafarizad, A.; Hacimuftuoglu, A.; Nikitovic, D.; Docea, A.O.; Mezhuev, Y.; Tsatsakis, A. Fe₃O₄ Nanoparticles in Combination with 5-FU Exert Antitumor Effects Superior to Those of the Active Drug in a Colon Cancer Cell Model. *Pharmaceutics* **2023**, *15*, 245. <https://doi.org/10.3390/pharmaceutics15010245>

Academic Editor: Qingxin Mu

Received: 27 November 2022

Revised: 5 January 2023

Accepted: 7 January 2023

Published: 11 January 2023



Copyright: © 2023 by the authors. Licensee MDPI, Basel, Switzerland. This article is an open access article distributed under the terms and conditions of the Creative Commons Attribution (CC BY) license (<https://creativecommons.org/licenses/by/4.0/>).

1. Introduction

Colon cancer is the third most common malignancy and represents the second most common cause of cancer death despite advances in diagnosis and treatment [1]. One of the key distinguishing features of colon cancer is the loss of cellular organization and the increased ability to invade near and distant sites. The standard treatment principle encompasses chemotherapy, surgery, and radiotherapy according to the type and stage of the disease. However, the gene-type signature of the cancer tissue alters the neoplasm response to therapy regimens [2]. Thus, the 5-year survival of colon cancer patients remains at 64%, and efficient therapy, with attenuated side effects, remains a significant unmet health need [3].

5-Fluorouracil (5-FU), an antineoplastic agent, is used to treat colon cancer by inhibiting the S phase of the cell cycle, thereby blocking DNA synthesis and triggering cell death [4,5]. However, due to its short half-life (5–14 min), poor membrane permeability, and rapid metabolism, high doses must be continuously administered to maintain a minimum therapeutic serum concentration, which often entails numerous side effects and severe toxicity [6–8]. Indeed, chemotherapeutics that prevent DNA synthesis can incur lethal side effects in rapidly dividing healthy tissues, including intestinal epithelium and blood cells [9].

Numerous studies have demonstrated that NPs significantly increase the drug uptake of cancer cells, thus improving the limitations of current chemotherapeutic agents [10]. Different metal NPs, including Au, TiO₂, Fe₃O₄, Pt, ZnO, and Mg NPs, were previously tested in various cancer models [11,12]. In addition, Fe₃O₄ nanoparticles (Fe₃O₄-NPs), or magnetite NPs, exhibit magnetic properties and have lately received approval from the Food and Drug Administration (FDA) for utilization in magnetic resonance imaging (MRI) [13].

Notably, metal NPs can enhance the accumulation of active drugs in a passive and active manner. For example, cancer tissues exhibit leaky vasculature with pore sizes reaching hundreds of nanometers, which enables the passive accumulation of inert metal NPs [14]. This mechanism is called the increased permeability and retention (EPR) effect. Furthermore, introducing functional modifications on the metal NP's surface will result in specific tissue targeting [15]. Indeed, incorporating specific ligands for tumor targeting, including peptides, antibodies, glycans, or folic acid, can increase drug release to tumor cells [16].

Notably, in some models, Fe₃O₄ metal oxides and their various composites [17,18] exhibit cytotoxic and genotoxic properties, resulting in DNA fragmentation, disturbance in the integrity of the mitochondrial membrane, and cell necrosis, as well as alterations in oncogene expression.

Furthermore, Fe₃O₄/composite nanomaterials enhanced reactive oxygen species (ROS) production and oxidative stress-inducing cell apoptosis [19]. Another exciting aspect of iron oxide action is its immunomodulatory effects. Thus, the inflammatory response of neutrophils in a vascular mimetic model is attenuated upon the uptake of iron oxide NPs [20]. Cytokines play a critical role in regulating the host cell's immune response to cancer and the mechanism of tumorigenesis [21]. Interleukin-10 (IL-10), an important cytokine secreted by various cell types, including macrophages, monocytes, neutrophils, and endothelial cells [22], was shown to affect the homeostasis of the intestinal epithelium. Notably, IL-10 is a crucial inhibitor of the immune response harnessed by various tumors to evade the immune system [19,23,24].

Phosphatase and tensin homolog (PTEN) is a protein tyrosine phosphatase expressed in humans [25]. PTEN has been characterized as a key tumor suppressor gene due to its ability to downregulate phosphatidylinositol 3-kinase (PI3K) and downstream Akt/mTOR signaling crucial to the modulation of cell growth [26,27]. Furthermore, both loss and partial/complete inactivation of PTEN expression have been identified in many cancers, allowing its characterization as an oncogene [27]. Indeed, PTEN inactivation/loss is one of the most frequent genetic alterations in sporadic cancer [27]. Heterogeneous PTEN hamartoma tumor syndrome (PHTS), due to pathogenic variants in the PTEN onco-suppressor gene, strongly correlates with colon cancer incidence [28]. Notably, in vivo colon cancer models demonstrated that efficient anticancer therapy increased PTEN expression [29].

In the current study, we evaluated the effects of the Fe₃O₄-NPs + 5-FU combination on cell viability, oxidative stress, cytokine, and oncogene expression in a Caco-2 colon cancer cell model. Our data demonstrated that the Fe₃O₄-NPs + 5-FU combination exerts anticancer effects at concentrations at which the active drug, 5-FU, is ineffective. Furthermore, this article shows that the combined administration of Fe₃O₄ nanoparticles with 5-FU without its prior immobilization significantly increased the antitumor activity and reduced the therapeutic dose of 5-FU.

2. Materials and Methods

2.1. Chemicals and Reagents

5-FU was obtained from Deva A.S (Istanbul, Turkey). Fe (acac)₃, phosphate-buffered solution (PBS), Dulbecco's modified Eagle's medium (DMEM), fetal bovine serum (FBS), trypsin (with EDTA), antibiotic, oleyl amine, and dibenzyl ether were supplied by Sigma-Aldrich (St. Louis, MO, USA).

2.2. Fe₃O₄ Nanoparticles Synthesis

Iron (III) acetylacetonate (Fe (acac)₃, 1.06 g) was dissolved in a mixture of oleyl amine (15 mL) and dibenzyl ether (15 mL) under continuous stirring in a four-necked round-bottom glass reactor. The mixture was heated to 120 °C and held at the same temperature for 1 h to remove moisture under a stream of nitrogen gas. The mixing process continued throughout all stages. After one hour, the mixture temperature was rapidly increased to 300 °C, and the reaction was continued at this temperature for an 1 h. Finally, ethanol (3 × 40 mL) was added to the mixture, which was centrifuged at 8500 rpm for 12 min. After purification, Fe₃O₄ NPs were dispersed in hexane (10 mL). Figure 1B shows a representative SEM image of the prepared Fe₃O₄ NPs [30,31].

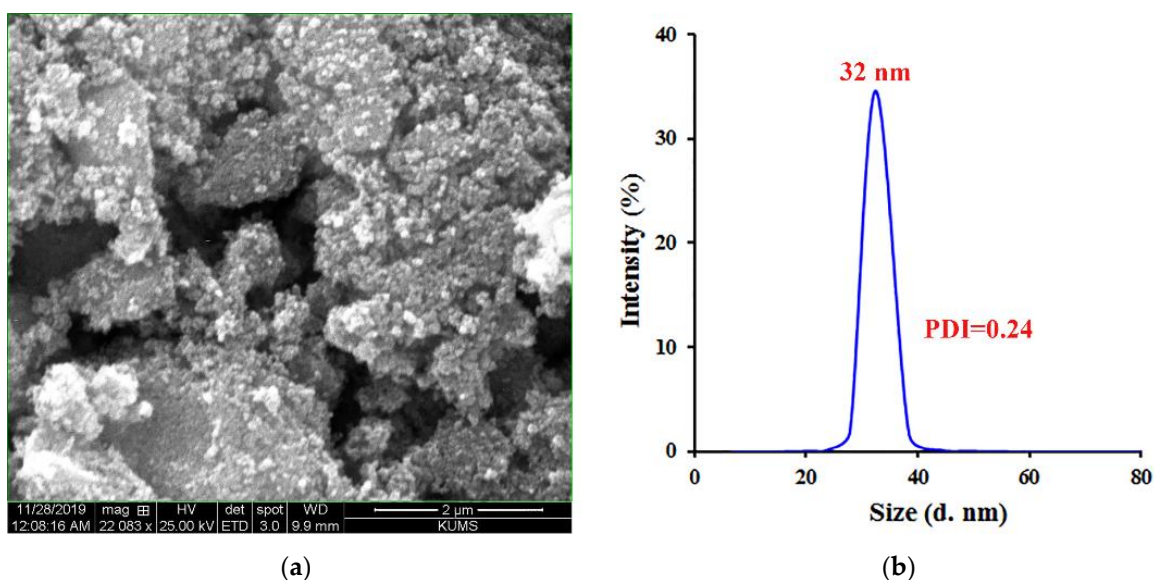


Figure 1. The (a) SEM image and (b) DLS analysis of Fe₃O₄ NPs.

2.3. Fe₃O₄ Nanoparticles Characterization

The scanning electron microscope (SEM) images were obtained using an FEI Quanta 450 (USA). Dynamic light scattering (DLS) experiments were performed utilizing a Zetasizer Quanta Nano ZS90 (Malvern Instruments, Malvern, UK) at room temperature. Samples were prepared as 0.5% (*w/v*) solutions in DDW.

The Fourier transform infrared (FTIR) spectrum of the Fe₃O₄ NPs was obtained with a Shimadzu 8101 M FTIR (Kyoto, Japan) using the potassium bromide (KBr) pellet technique. The powder X-ray diffraction (XRD) pattern of the Fe₃O₄ NPs was obtained using a Siemens D5000 diffractometer (Aubrey, TX, USA) and an X-ray generator (CuK α radiation with $\lambda = 1.5406 \text{ \AA}$) at room temperature [31].

2.4. Cell Cultures

2.4.1. Caco-2 Cell Culture

Caco-2 (HTB-37TM) cells were obtained from ATCC. The cells were cultured in DMEM (1% antibiotic (amphotericin B, penicillin, and streptomycin) and 10% FBS), and held at the optimum conditions (5% CO₂; 37 °C).

2.4.2. Cell Treatments

After the cells reached 85% confluency, they were harvested and seeded in 96-well plates (Corning, Corning, NY, USA) [32]. Treatments were determined as control, Fe₃O₄ NPs 6 µg/mL, 5-FU (4, 8, and 16 µg/mL), and a combination (Fe₃O₄ NPs + 5-FU). The cells were exposed to the various treatments for 24 or 72 h.

2.5. MTT Assay

At the end of the experiment (after 24 and 72 h of treatment), MTT solution (10 µL) was added to each well, and the cell number was determined. In short, the plates were incubated for 4 h in a CO₂ incubator, to which 100 µL of DMSO solution was added to all wells. The spectrophotometer read the density at 570 nm [31].

2.6. Total Oxidant Status (TOS) and Total Antioxidant Capacity (TAC) Determination

Total oxidant status (TOS) and total antioxidant capacity (TAC) evaluations were performed spectrophotometrically (Multiskan™ GO Microplate Spectrophotometer reader) as previously described [26]. The color density is correlated to the oxidant levels in a sample [33].

2.7. Lactate Dehydrogenase (LDH) Measurement

According to the manufacturer's instructions, the lactate dehydrogenase (LDH) was determined with an LDH detection kit. In summary, Caco-2 cells were seeded in a 96-well plate at a density of 10³–10⁶ cells/well in 200 µL of the medium. Six wells were prepared for each concentration. Triton X-100 (10%) and the assay buffer were added, and the wells were incubated at room temperature for one hour. After centrifugation, the cell supernatant was transferred to a new 96-well assay plate. The LDH reaction solution was added to each well, and the plate was incubated with gentle shaking on an orbital shaker for 30 min at 37 °C. A microplate reader measured the absorbance OD value at 490 nm [34]. ((experimental value A490) – (spontaneous release A490))/((maximum release A490) – (spontaneous release A490)) × 100.

Maximum release: 100% dead cells by adding Triton X-100.

Spontaneous release: nontoxic materials (cell medium) control group.

Experiment value: application groups.

2.8. Gene Expression Determination

The total RNA from Caco-2 cells was used to synthesize complementary DNA (cDNA) using a high-capacity cDNA Reverse Transcription Kit. The sequences of the gene-specific PCR primers are listed below (forward and reverse). Results were compared with the control group and are expressed as relative fold. Gene expressions were normalized to beta actin using the $\Delta\Delta$ Ct method.

Beat actin: CCAACCGCGAGAAGATGA'; CCAGAGGCGTACAGGGATAG'

PTEN: TGAGTTCCTCAGCCGTTACCT'; GAGGTTTCCTCTGGTCCTGGTA'

IL-1β: TCTCAGATTCACAACCTGTTCTGTG'; AGAAAATGAGGTCGGTCTCACTA'

IL-10: GGCATGCTTGGCTCAGCACTG-3'; GCCCTGCAGTCCAGTAGACG'

2.9. Statistical Analyses

Statistical comparisons between the groups were calculated using one-way ANOVA and Tukey's HSD method. All calculations were performed using SPSS 20 software for statistical analysis, and a $p < 0.05$ was considered a statistically significant difference in all tests. Results are presented as mean and standard deviation (mean ± SD).

3. Results

3.1. Characterization of Fe₃O₄ NPs

The synthesized Fe₃O₄ NPs were characterized using SEM and DLS analysis, as presented in Figure 1. The SEM image showed that the shape of the synthesized Fe₃O₄

NPs was spherical with an average diameter of 35 ± 5 nm. The DLS analysis revealed that the Fe_3O_4 NPs had an average size of ~ 32 nm. In addition, the polydispersity index (PDI) of the synthesized NPs was found to be 0.24, which indicated their relatively monodisperse synthesis.

The FTIR spectrum and XRD pattern of the Fe_3O_4 NPs are shown in Figure 2. The most prominent absorption bands in the FTIR spectrum are the stretching vibration of the metal–oxygen (Fe–O) group at 576 cm^{-1} and the stretching and bending vibrations of the surface hydroxyl groups at 3420 and 1608 cm^{-1} , respectively (Figure 2a).

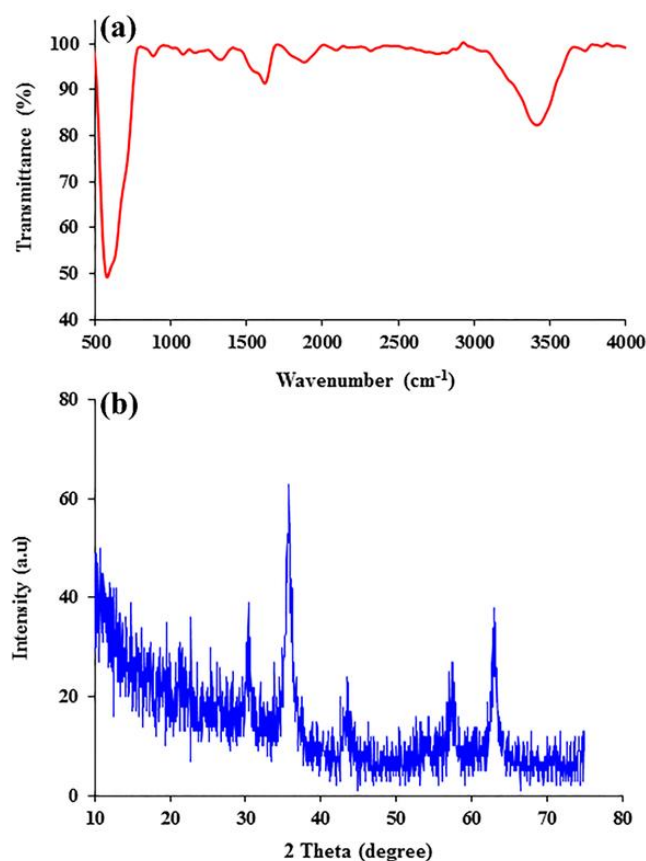


Figure 2. FTIR spectrum (a) and XRD pattern (b) of Fe_3O_4 NPs.

The crystallographic analysis of the synthesized Fe_3O_4 NPs was performed by XRD analysis, as depicted in Figure 2b. In the XRD model of Fe_3O_4 NPs, the characteristic peaks belonging to the XRD spectrum at $2\theta = 30.6^\circ$, 36.1° , 43.1° , 52.6° , 57.7° , and 63.1° can be indexed at (220), (311), (400), (422), (511), and (440), respectively. This FTIR spectrum and XRD pattern confirm the successful synthesis of Fe_3O_4 -NPs.

3.2. Evaluation of Caco-2 Cell Viability by MTT and LDH Assay

The effect of various treatments on Caco-2 cell viability was determined by the MTT assay after 24 and 72 h of treatment (Figure 3). Cell viability was considered as 100% in the control (negative control) and is expressed as a percentage of that of the control for all other treatments. Notably, DMSO and the nonloaded Fe_3O_4 NPs at $6\text{ }\mu\text{g/mL}$ did not affect the viability of Caco-2 cells. Treating the cells for 24 h with 5-FU $16\text{ }\mu\text{g/mL}$ exerted a nonsignificant 10% decrease in viability ($p = \text{NS}$), and the reduction (34%) was statistically significant after 72 h of treatment ($p < 0.05$). The effects of the Fe_3O_4 -NPs + 5-FU combination on cell viability were more prominent. Thus, treating cells for 24 h with Fe_3O_4 NPs + 5-FU ($16\text{ }\mu\text{g/mL}$) decreased their viability to 31% ($p < 0.05$), whereas treating Caco-2 cells with Fe_3O_4 NPs + 5-FU ($16\text{ }\mu\text{g/mL}$) for 72 h resulted in a substantial decrease in their viability (41%) ($p < 0.01$).

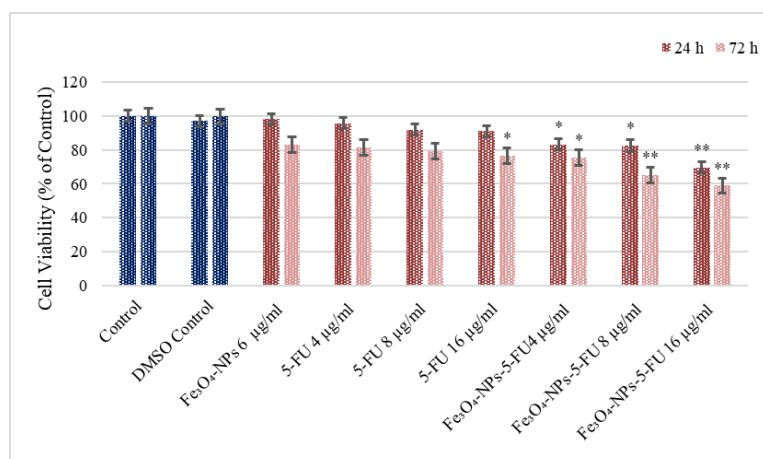


Figure 3. Cell viability was measured with an MTT assay ($n = 6$). The effect of Fe₃O₄-NPs, 5-FU, and Fe₃O₄-NPs + 5-FU on Caco-2 cells' viability. Cells were cultured in 96-well plates and treated with Fe₃O₄-NPs 6 µg/mL, 5-FU (4, 8, and 16 µg/mL), and the Fe₃O₄ NPs + 5-FU combination for 24 h and 72 h. The results are presented as the average of three separate experiments. Statistical significance: * $p < 0.05$; ** $p < 0.01$.

Because LDH is released by necrotic cells, it is an excellent metabolic marker of cell viability. The effect of various treatments on Caco-2 cell LDH activity was determined by utilizing an LDH kit (Figure 3). The measured LDH activity of treated cells expressed as a percent of the standard (designated as 100%) is presented in Figure 4. Treating the cells with only Fe₃O₄-NPs and different concentrations of 5-FU did not affect their LDH activity. However, an increase in LDH activity, correlated with cell death, was demonstrated in cells treated with a combination of Fe₃O₄-NPs + 5-FU (8 µg/mL) for 72 h ($p < 0.05$) and cells treated with Fe₃O₄-NPs + 5FU (16 µg/mL) for 24 and 72 h, ($p < 0.05$ and $p < 0.01$), respectively. These data demonstrate that combining 5FU with Fe₃O₄-NPs significantly increased the active drug cytotoxic effect, even at concentrations below the active drug range.

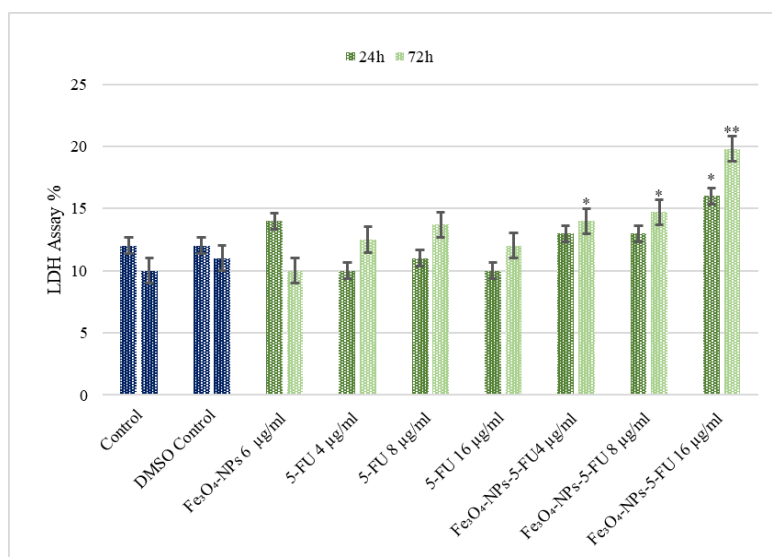


Figure 4. The effect of Fe₃O₄-NPs, 5-FU, and Fe₃O₄-NPs + 5-FU on Caco-2 cell LDH activity ($n = 6$). Cells were cultured in 96-well plates and treated with Fe₃O₄-NPs 6 µg/mL, 5-FU (4, 8, and 16 µg/mL), and combinations of Fe₃O₄ + 5-FU NPs for 24 h and 72 h, and LDH activity was determined. The results represent the average of three separate experiments. Statistical significance is represented as * $p < 0.05$; ** $p < 0.01$.

3.3. The Effect of Fe₃O₄-NPs, 5-FU and Fe₃O₄-NPs + 5-FU on Caco-2 Cells Redox State

The Caco-2 cell TAC values, determined spectrophotometrically, were 12.01 and 13.84 mmol Trolox equiv/L, respectively (Figure 5). Treatment with Fe₃O₄ NPs, and different concentrations of 5-FU did not affect these cells' TAC. However, treatment with the loaded Fe₃O₄-NPs + 5-FU significantly decreased the Caco-2 cell antioxidant status in a time- and concentration-dependent manner (Figure 5).

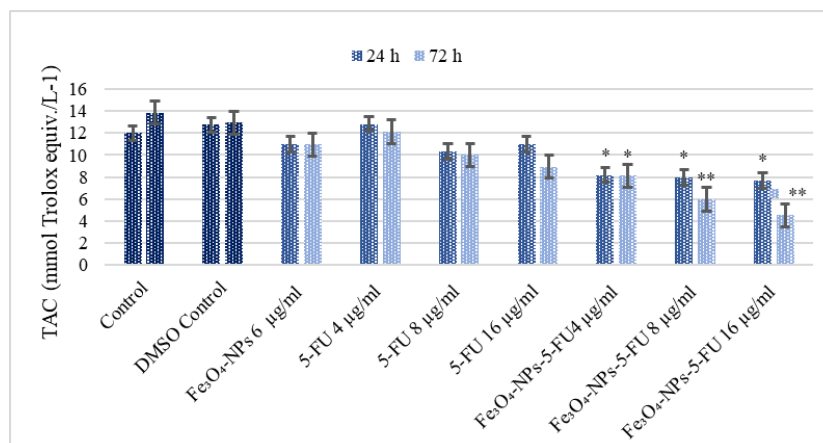


Figure 5. The effect of Fe₃O₄-NPs, 5-FU, and Fe₃O₄-NPs + 5-FU on Caco-2 cells' TAC (n = 6). Cells were cultured in 96-well plates and treated with Fe₃O₄ NPs 6 µg/mL, 5-FU (4, 8, and 16 µg/mL), and Fe₃O₄ + 5-FU NPs combinations for 24 h and 72 h, and TAC determined. The results represent the average of three separate experiments. Statistical significance: * *p* < 0.05; ** *p* < 0.01.

In correlation with the TAC results, the combined Fe₃O₄-NPs + 5-FU treatments (Figure 6) was found to increase Caco-2 cell TOS levels, dependent on time and concentration. The most pronounced effects were obtained after 72 h of treatment with Fe₃O₄-NPs + 5U 8 µg/mL/5-FU 16 µg/mL (*p* < 0.01).

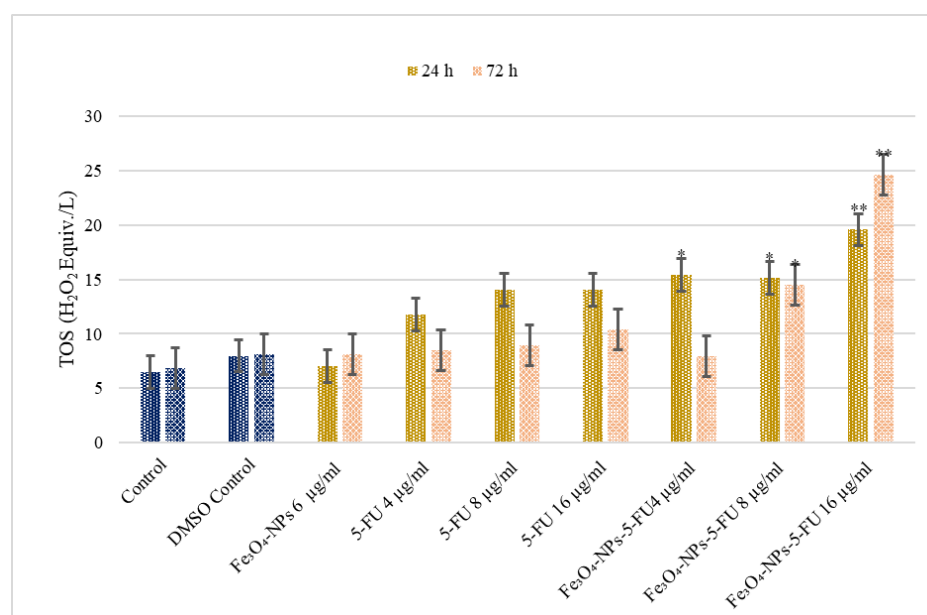


Figure 6. The effect of Fe₃O₄-NPs, 5-FU, and Fe₃O₄-NPs + 5-FU on Caco-2 cells TOS levels (n = 6). Cells were cultured in 96-well plates and treated with Fe₃O₄-NPs 6 µg/mL, 5-FU (4, 8, and 16 µg/mL), and combinations of Fe₃O₄ + 5-FU NPs for 24 h and 72 h, and TOS determined. The results represent the average of three separate experiments. Statistical significance: * *p* < 0.05; ** *p* < 0.01.

3.4. The Effect of Fe₃O₄-NPs, 5-FU and Fe₃O₄-5-FU NPs on PTEN and IL-10 Gene Expression

PTEN and IL-10 gene expression levels were measured with real-time PCR analysis at the 72 h point of various treatments. This approach demonstrated that the Fe₃O₄-NPs + 5-FU (8 µg/mL) and Fe₃O₄-5-NPs + FU (16 µg/mL) treatments significantly up-regulated PTEN expression ($p < 0.05$ and $p < 0.01$, respectively). A 1.34-fold increase for the Fe₃O₄-NPs + 5-FU (8 µg/mL) and a 1.57-fold for the Fe₃O₄-NPs + 5-FU (16 µg/mL) treatments were determined (Figure 7a).

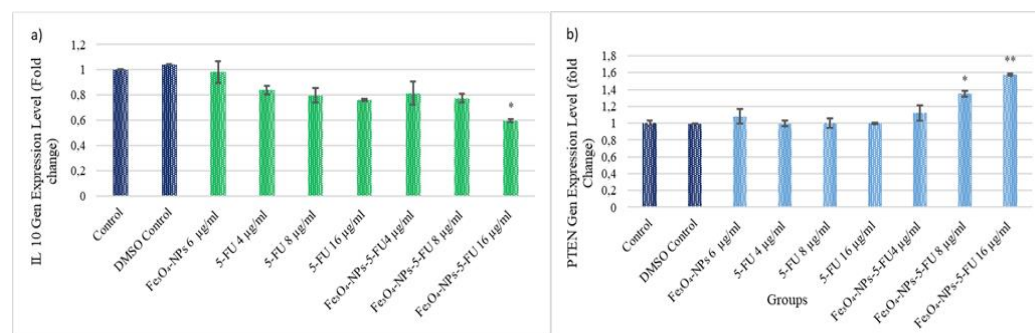


Figure 7. The effect of Fe₃O₄-NPs, 5-FU, and Fe₃O₄-NPs + 5-FU on PTEN and IL-10 gene expression. (a) IL-10 gene level; (b) PTEN gene level (n = 3). Cells were cultured in 96-well plates and treated with Fe₃O₄-NPs 6 µg/mL, 5-FU (4, 8, and 16 µg/mL), and combinations of Fe₃O₄ + 5-FU NPs for 72 h. The results represent the average of three separate experiments. Statistical significance: * $p < 0.05$; ** $p < 0.01$.

On the other hand, the expression of the immunosuppressive IL-10 gene level was significantly downregulated in Caco-2 cells exposed to Fe₃O₄-NPs + 5-FU (16 µg/mL), with a 0.59 decrease ($p < 0.05$) (Figure 7b).

4. Discussion

Over the past decades, remarkable advances have occurred in nanotechnology, particularly nanomedicine, focusing, among others, on novel cancer therapeutics [35]. NPs can accumulate in cells without being recognized by *p*-glycoproteins, one of the primary mediators of multidrug resistance, resulting in increased intracellular concentrations of drugs [36]. Notably, NP carriers exhibit intrinsic abilities affecting cancer and immune cell biological functions [37]. Therefore, our study examined the synergistic effect of Fe₃O₄-NPs and 5-FU on Caco-2 colon cancer cell viability, oxidative stress, and oncogene expression.

Previous studies have shown an ambiguous effect of iron oxide NPs on cell biological functions, dependent on cell type and concentration utilized. Thus, it was shown that iron oxide NPs could induce the cellular inflammatory response and increase the secretion of proinflammatory cytokines in human or mouse cells [37,38]. Lately, they have been approved by the FDA, and their beneficial effects on cell physiology have been suggested [13]. However, Fe₃O₄/composites were also shown to facilitate various active drugs' cytotoxic and immunomodulatory properties [39]. Thus, the peroxidase-like activity of Fe₃O₄ and carbon NPs was found to facilitate ascorbic-acid-induced oxidative stress and to incur specific damage to PC-3 prostate cancer cells [40]. Furthermore, increased ROS production generates oxidative stress within the cells and cell apoptosis, resulting in PC-3 tumor cell growth inhibition [40]. Moreover, composite NPs can induce mitochondrial membrane alteration, DNA damage, cytokine production associated with oxidative stress, and apoptosis-correlated cell death [41].

A separate research direction is the regulation of magnetic fields, as various studies have shown that the discrete modulation of these fields can inhibit the proliferation of cancer cells and tumor growth [42,43]. Furthermore, due to the promoting effect of iron metabolism on ROS production, increased concentrations of iron-based NPs in cancer cells enhance their exposure to the local magnetic field and cellular death [44,45].

Our study showed that Fe₃O₄ NPs did not negatively affect Caco-2 cell viability, oxidative stress, or oncogene expression. However, together with 5-FU, Fe₃O₄ NPs acted synergistically, and the combination exerted cytotoxic, immunomodulatory, and oxidative-stress-promoting effects at a concentration at which the active drug does not affect these cell functions. Notably, LDH is a cytotoxic marker as its release is enhanced due to cell necrosis. In this study, combined Fe₃O₄-NPs + 5-FU strongly increased LDH activity, correlated with the upregulation of cell death. Furthermore, TOS increase and TAC attenuation were evident after combined Fe₃O₄-NPs + 5-FU treatment. Notably, the effects were exerted only after combined Fe₃O₄-NPs + 5-FU treatment, as treating cells with only 5-FU at the same concentrations did not affect these parameters of cell homeostasis.

PTEN is a well-established tumor suppressor, and alterations in its expression/activity are correlated with tumorigenesis [46]. Moreover, as PTEN controls polarity in normal epithelial cells, loss of this protein plays a critical role in the invasion and metastasis of various cancer types, including colon cancer [47,48]. Several studies have established a negative correlation of PTEN expression with colon cancer progression due to its vital role in inhibiting the malignant transformation of intestinal epithelial cells [49]. A similar association was determined with the dysregulation of PTEN-binding partners [50–52]. In the present study, the combined Fe₃O₄-NPs + 5-FU significantly increased this gene expression. Notably, PTEN acts as a negative regulator of the PI3K/Akt signaling pathway and was shown to affect many processes deregulated in tumorigenesis, such as cell survival, proliferation, migration, and invasion [53]. Indeed, inhibition of the PI3K/Akt pathway induces programmed cell death in different cell lines [54]. Recently, patients presenting PTEN hamartoma tumor syndrome were advised to employ earlier surveillance for colon cancer due to an increased risk of early onset [55]. In the present study, Fe₃O₄-NPs in combination with 5-FU increased PTEN gene expression. Moreover, in an *in vivo* prostate cancer model, a NP-mediated increase in PTEN led to disease remission, highlighting the importance of this gene in tumorigenesis and defining it as a promising therapeutic target and progression marker [56].

IL-10 is a versatile immunosuppressive cytokine with immunomodulatory functions [20]. Thus, IL-10 increases tumor cell survival, proliferation, and metastasis by controlling antitumor immunity. Indeed, IL-10 exerts suppressive effects on effector immune cells, including potent antitumor cytotoxic NK and CD8 T cells [21]. The immunosuppressive functions of IL-10 are exercised through the Jak1/STAT3 pathway. Moreover, IL-10 suppresses the level of proinflammatory cytokines, including IL-1 β [57]. IL-10 exhibits a role in colon cancer progression as increased levels of IL-10 facilitated liver metastasis in a mouse model [55]. Reprogramming the colon cancer tumor environment by silencing IL-10 expression resulted in dendritic-cell-dependent activation of the antitumor response [56]. This is a significant achievement, especially as dendritic cells (DCs) have a key role in triggering antitumor immune responses [58]. Madhubala et al. [59], in their study on titanium dioxide NPs' effects in a leukemia cell line, observed that the expression of IL-10 significantly decreased. In the present study, Fe₃O₄-NPs + 5-FU treatment significantly reduced the IL-10 release of colon cancer cells.

Thus, this study shows that the combined administration of Fe₃O₄ and 5-FU NPs will reduce the dose of the drug required to achieve pronounced antitumor activity. The latter effect is a significant result since 5-FU has a pronounced toxicity, which can be reduced due to its immobilization, for example, using metal–organic frameworks [60–62]. Therefore, the role of NPs is not only to provide suitable dynamics for 5-FU release in the event of its immobilization but also to eliminate the barrier associated with penetration through the cell membrane. A similar synergistic effect was described when platinum NPs were administered together with nonimmobilized doxorubicin to U2OS osteosarcoma cells. In this model, cotreatment significantly increased the drug's effectiveness compared with pure doxorubicin at a similar dose [63]. This was explained by an increase in oxidative stress in the presence of platinum NPs [63], which we also noted with the combined introduction of Fe₃O₄ and 5-FU nanoparticles in the present study. On the other hand, NP treatment

promotes the activation of endocytosis [64], which can also promote the penetration of 5-FU through cell membranes. Therefore, administering anticancer drugs, even without their preliminary immobilization, together with NPs, can significantly increase their cytostatic activity. Furthermore, in vivo and in vitro experiments for the characterization of Fe₃O₄ nanoparticles/active drug effects on specific cells/tissues are in order.

5. Conclusions

Magnetite NPs penetrate (passive delivery) due to increased vascular permeability and weakened lymphatic drainage of cancer tissues. Moreover, magnetite NPs are easily uptaken and accumulate in cancer cells due to their small size. Our study showed that the combined Fe₃O₄-NPs + 5-FU, through a synergistic effect, significantly reduced Caco-2 cell viability at a concentration at which the active drug did not induce an effect. Likewise, the combined treatment, but not the solitary components, facilitated oxidative stress correlated with the decreased viability of Caco-2 cells. Moreover, we determined that combined Fe₃O₄-NPs + 5-FU treatment decreased IL-10 levels and enhanced the expression of the oncogene-suppressor PTEN. Our data show that Fe₃O₄-NPs + 5-FU exhibit significant antitumor effects at low concentrations of the active drug. Further studies are needed to fully elucidate the molecular mechanisms involved.

Author Contributions: S.G., A.T. (Ali Taghizadehghalehjoughi), Y.Y., A.H., A.O.D. and A.T. (Aristidis Tsatsakis): conceptualization, methodology, supervision, investigation, writing—review and editing. A.J., D.N. and Y.M.: software, validation, formal analysis, investigation, data curation, writing—original draft preparation. A.J., S.G. and Y.Y.: resources. All authors have read and agreed to the published version of the manuscript.

Funding: This research received no external funding.

Institutional Review Board Statement: Not applicable.

Informed Consent Statement: Not applicable.

Data Availability Statement: Raw data is available on request.

Conflicts of Interest: The authors declare no conflict of interest.

References

1. Siegel, R.L.; Miller, K.D.; Jemal, A. Cancer statistics, 2018. *CA Cancer J. Clin.* **2018**, *68*, 7–30. [[CrossRef](#)]
2. Alfaro, A.E.A.; Castillo, B.M.; Garcia, E.C.; Tascon, J.; Morales, A.I. Colon Cancer Pharmacogenetics: A Narrative Review. *Pharmacy* **2022**, *10*, 95. [[CrossRef](#)]
3. Li, Y.; Gao, Y.; Gong, C.N.; Wang, Z.; Xia, Q.M.; Gu, F.F.; Hu, C.L.; Zhang, L.J.; Guo, H.L.; Gao, S. A33 antibody-functionalized exosomes for targeted delivery of doxorubicin against colorectal cancer. *Nanomed. Nanotechnol. Biol. Med.* **2018**, *14*, 1973–1985. [[CrossRef](#)]
4. Krishna, R.; Mayer, L.D. Multidrug resistance (MDR) in cancer—Mechanisms, reversal using modulators of MDR and the role of MDR modulators in influencing the pharmacokinetics of anticancer drugs. *Eur. J. Pharm. Sci.* **2000**, *11*, 265–283. [[CrossRef](#)]
5. Anitha, A.; Deepa, N.; Chennazhi, K.P.; Lakshmanan, V.K.; Jayakumar, R. Combinatorial anticancer effects of curcumin and 5-fluorouracil loaded thiolated chitosan nanoparticles towards colon cancer treatment (vol 1840, pg 2730, 2014). *Biochim. Biophys. Acta-Gen. Subj.* **2019**, *1863*, 992. [[CrossRef](#)]
6. Zhang, J.X.; Yang, Z.R.; Wu, D.D.; Song, J.; Guo, X.F.; Wang, J.; Dong, W.G. Suppressive Effect of Sinomenine Combined with 5-Fluorouracil on Colon Carcinoma Cell Growth. *Asian Pac. J. Cancer Prev.* **2014**, *15*, 6737–6743. [[CrossRef](#)]
7. Baker, E.K.; El-Osta, A. The rise of DNA methylation and the importance of chromatin on multidrug resistance in cancer. *Exp. Cell Res.* **2003**, *290*, 177–194. [[CrossRef](#)]
8. Comella, P.; Casaretti, R.; Sandomenico, C.; Avallone, A.; Franco, L. Capecitabine, alone and in combination, in the management of patients with colorectal cancer—A review of the evidence. *Drugs* **2008**, *68*, 949–961. [[CrossRef](#)]
9. Hossen, S.; Hossain, M.K.; Basher, M.K.; Mia, M.N.H.; Rahman, M.T.; Uddin, M.J. Smart nanocarrier-based drug delivery systems for cancer therapy and toxicity studies: A review. *J. Adv. Res.* **2019**, *15*, 1–18. [[CrossRef](#)]
10. Tang, Q.C.; Wang, Y.H.; Huang, R.; You, Q.; Wang, G.Y.; Chen, Y.G.; Jiang, Z.; Liu, Z.; Yu, L.; Muhammad, S.; et al. Preparation of Anti-Tumor Nanoparticle and Its Inhibition to Peritoneal Dissemination of Colon Cancer. *PLoS ONE* **2014**, *9*, e98455. [[CrossRef](#)]
11. Chaturvedi, V.K.; Singh, A.; Singh, V.K.; Singh, M.P. Cancer Nanotechnology: A New Revolution for Cancer Diagnosis and Therapy. *Curr. Drug Metab.* **2019**, *20*, 416–429. [[CrossRef](#)]

12. Mioc, M.; Pavel, I.Z.; Ghiulai, R.; Coricovac, D.E.; Farcas, C.; Mihali, C.V.; Oprean, C.; Serafim, V.; Popovici, R.A.; Dehelean, C.A.; et al. The Cytotoxic Effects of Betulin-Conjugated Gold Nanoparticles as Stable Formulations in Normal and Melanoma Cells. *Front. Pharmacol.* **2018**, *9*, 429. [[CrossRef](#)]
13. Chen, Y.L.; Hou, S.K. Application of magnetic nanoparticles in cell therapy. *Stem Cell Res. Ther.* **2022**, *13*, 135. [[CrossRef](#)]
14. Lok, C.N.; Zou, T.T.; Zhang, J.J.; Lin, I.W.S.; Che, C.M. Controlled-Release Systems for Metal-Based Nanomedicine: Encapsulated/Self-Assembled Nanoparticles of Anticancer Gold(III)/Platinum(II) Complexes and Antimicrobial Silver Nanoparticles. *Adv. Mater.* **2014**, *26*, 5550–5557. [[CrossRef](#)]
15. Darroudi, M.; Gholami, M.; Rezayi, M.; Khazaei, M. An overview and bibliometric analysis on the colorectal cancer therapy by magnetic functionalized nanoparticles for the responsive and targeted drug delivery. *J. Nanobiotechnol.* **2021**, *19*, 399. [[CrossRef](#)]
16. Perez-Herrero, E.; Fernandez-Medarde, A. Advanced targeted therapies in cancer: Drug nanocarriers, the future of chemotherapy. *Eur. J. Pharm. Biopharm.* **2015**, *93*, 52–79. [[CrossRef](#)]
17. Kaplan, A.; Kutlu, H.M.; Ciftci, G.A. Fe₃O₄ Nanopowders: Genomic and Apoptotic Evaluations on A549 Lung Adenocarcinoma Cell Line. *Nutr. Cancer* **2020**, *72*, 708–721. [[CrossRef](#)]
18. Li, D.; Deng, M.W.; Yu, Z.Y.; Liu, W.; Zhou, G.D.; Wang, X.S.; Yang, D.P.; Zhang, W.J. Biocompatible and Stable GO-Coated Fe₃O₄ Nanocomposite: A Robust Drug Delivery Carrier for Simultaneous Tumor MR Imaging and Targeted Therapy. *ACS Biomater. Sci. Eng.* **2018**, *4*, 2143–2154. [[CrossRef](#)]
19. Zhang, Y.L.; Zhang, Y.T.; Yang, Z.J.; Fan, Y.; Chen, M.Y.; Zhao, M.T.; Dai, B.; Zheng, L.L.; Zhang, D.W. Cytotoxicity Effect of Iron Oxide (Fe₃O₄)/Graphene Oxide (GO) Nanosheets in Cultured HBE Cells. *Front. Chem.* **2022**, *10*, 888033. [[CrossRef](#)]
20. Garcia, G.; Kim, M.H.; Morikis, V.A.; Simon, S.I. Neutrophil Inflammatory Response Is Downregulated by Uptake of Superparamagnetic Iron Oxide Nanoparticle Therapeutics. *Front. Immunol.* **2020**, *11*, 571489. [[CrossRef](#)]
21. Propper, D.J.; Balkwill, F.R. Harnessing cytokines and chemokines for cancer therapy. *Nat. Rev. Clin. Oncol.* **2022**, *19*, 237–253. [[CrossRef](#)]
22. Germano, G.; Allavena, P.; Mantovani, A. Cytokines as a key component of cancer-related inflammation. *Cytokine* **2008**, *43*, 374–379. [[CrossRef](#)]
23. Zhang, H.Y.; Li, R.C.; Cao, Y.F.; Gu, Y.; Lin, C.; Liu, X.; Lv, K.P.; He, X.D.; Fang, H.J.; Jin, K.F.; et al. Poor Clinical Outcomes and Immuno-evasive Contexture in Intratumoral IL-10-Producing Macrophages Enriched Gastric Cancer Patients. *Ann. Surg.* **2022**, *275*, E626–E635. [[CrossRef](#)]
24. Ye, L.S.; Zhang, Q.; Cheng, Y.S.; Chen, X.L.; Wang, G.Y.; Shi, M.C.; Zhang, T.; Cao, Y.J.; Pan, H.; Zhang, L.T.; et al. Tumor-derived exosomal HMGB1 fosters hepatocellular carcinoma immune evasion by promoting TIM-1⁺ regulatory B cell expansion. *J. Immunother. Cancer* **2018**, *6*, 145. [[CrossRef](#)]
25. Steck, P.A.; Pershouse, M.A.; Jasser, S.A.; Yung, W.K.; Lin, H.; Ligon, A.H.; Langford, L.A.; Baumgard, M.L.; Hattier, T.; Davis, T.; et al. Identification of a candidate tumour suppressor gene, MMAC1, at chromosome 10q23.3 that is mutated in multiple advanced cancers. *Nat Genet* **1997**, *15*, 356–362. [[CrossRef](#)]
26. Fedorova, O.; Parfenyev, S.; Daks, A.; Shuvalov, O.; Barlev, N.A. The Role of PTEN in Epithelial-Mesenchymal Transition. *Cancers* **2022**, *14*, 3786. [[CrossRef](#)]
27. Papa, A.; Pandolfi, P.P. The PTEN(-)PI3K Axis in Cancer. *Biomolecules* **2019**, *9*, 153. [[CrossRef](#)]
28. D’Ermo, G.; Genuardi, M. Gastrointestinal manifestations in PTEN hamartoma tumor syndrome. *Best Pr. Res. Clin. Gastroenterol.* **2022**, *58–59*, 101792. [[CrossRef](#)]
29. Almaimani, R.A.; Aslam, A.; Ahmad, J.; El-Readi, M.Z.; El-Boshy, M.E.; Abdelghany, A.H.; Idris, S.; Alhadrami, M.; Althubiti, M.; Almasmoum, H.A.; et al. In Vivo and In Vitro Enhanced Tumoricidal Effects of Metformin, Active Vitamin D₃, and 5-Fluorouracil Triple Therapy against Colon Cancer by Modulating the PI3K/Akt/PTEN/mTOR Network. *Cancers* **2022**, *14*, 1538. [[CrossRef](#)]
30. Oh, G.W.; Kim, S.C.; Kim, T.H.; Jung, W.K. Characterization of an oxidized alginate-gelatin hydrogel incorporating a COS-salicylic acid conjugate for wound healing. *Carbohydr. Polym.* **2021**, *252*, 117145. [[CrossRef](#)]
31. Nalci, O.B.; Nadaroglu, H.; Genc, S.; Hacimuftuoglu, A.; Alayli, A. The effects of MgS nanoparticles-Cisplatin-bio-conjugate on SH-SY5Y neuroblastoma cell line. *Mol. Biol. Rep.* **2020**, *47*, 9715–9723. [[CrossRef](#)]
32. Kamalak, H.; Kamalak, A.; Taghizadehghalehjoughi, A.; Hacimuftuoglu, A.; Nalci, K.A. Cytotoxic and biological effects of bulk fill composites on rat cortical neuron cells. *Odontology* **2018**, *106*, 377–388. [[CrossRef](#)]
33. Cicek, B.; Genc, S.; Yeni, Y.; Kuzucu, M.; Cetin, A.; Yildirim, S.; Bolat, I.; Kantarci, M.; Hacimuftuoglu, A.; Lazopoulos, G.; et al. Artichoke (Cynara Scolymus) Methanolic Leaf Extract Alleviates Diethylnitrosamine-Induced Toxicity in BALB/c Mouse Brain: Involvement of Oxidative Stress and Apoptotically Related Klotho/PPARγ Signaling. *J. Pers. Med.* **2022**, *12*, 2012. [[CrossRef](#)]
34. Yeni, Y.; Cakir, Z.; Hacimuftuoglu, A.; Taghizadehghalehjoughi, A.; Okay, U.; Genc, S.; Yildirim, S.; Saglam, Y.S.; Calina, D.; Tsatsakis, A.; et al. A Selective Histamine H₄ Receptor Antagonist, JNJ7777120, Role on glutamate Transporter Activity in Chronic Depression. *J. Pers. Med.* **2022**, *12*, 246. [[CrossRef](#)]
35. Mundekkad, D.; Cho, W.L.C. Nanoparticles in Clinical Translation for Cancer Therapy. *Int. J. Mol. Sci.* **2022**, *23*, 1685. [[CrossRef](#)]
36. Mills, H.; Acquah, R.; Tang, N.V.; Cheung, L.; Klenk, S.; Glassen, R.; Pirson, M.; Albert, A.; Hoang, D.T.; Van, T.N. Preparation of PCL Electrospun Fibers Loaded with Cisplatin and Their Potential Application for the Treatment of Prostate Cancer. *Emerg. Med. Int.* **2022**, *2022*, 6449607. [[CrossRef](#)]

37. Zhu, M.T.; Wang, B.; Wang, Y.; Yuan, L.; Wang, H.J.; Wang, M.; Ouyang, H.; Chai, Z.F.; Feng, W.Y.; Zhao, Y.L. Endothelial dysfunction and inflammation induced by iron oxide nanoparticle exposure: Risk factors for early atherosclerosis. *Toxicol. Lett.* **2011**, *203*, 162–171. [[CrossRef](#)]
38. Park, E.J.; Choi, D.H.; Kim, Y.; Lee, E.W.; Song, J.; Cho, M.H.; Kim, J.H.; Kim, S.W. Magnetic iron oxide nanoparticles induce autophagy preceding apoptosis through mitochondrial damage and ER stress in RAW264.7 cells. *Toxicol. Vitro.* **2014**, *28*, 1402–1412. [[CrossRef](#)]
39. Zhao, S.Z.; Yu, X.J.; Qian, Y.N.; Chen, W.; Shen, J.L. Multifunctional magnetic iron oxide nanoparticles: An advanced platform for cancer theranostics. *Theranostics* **2020**, *10*, 6278–6309. [[CrossRef](#)]
40. An, Q.; Sun, C.Y.; Li, D.; Xu, K.; Guo, J.; Wang, C.C. Peroxidase-Like Activity of Fe₃O₄@Carbon Nanoparticles Enhances Ascorbic Acid-Induced Oxidative Stress and Selective Damage to PC-3 Prostate Cancer Cells. *ACS Appl. Mater. Interfaces* **2013**, *5*, 13248–13257. [[CrossRef](#)]
41. Alarifi, S.; Ali, D.; Alakhtani, S.; Al Suhaibani, E.S.; Al-Qahtani, A.A. Reactive Oxygen Species-Mediated DNA Damage and Apoptosis in Human Skin Epidermal Cells After Exposure to Nickel Nanoparticles. *Biol. Trace Elem. Res.* **2014**, *157*, 84–93. [[CrossRef](#)] [[PubMed](#)]
42. Choi, J.W.; Park, J.W.; Na, Y.; Jung, S.J.; Hwang, J.K.; Choi, D.; Lee, K.G.; Yun, C.O. Using a magnetic field to redirect an oncolytic adenovirus complexed with iron oxide augments gene therapy efficacy. *Biomaterials* **2015**, *65*, 163–174. [[CrossRef](#)]
43. Wang, S.H.; Luo, J.; Zhang, Z.H.; Dong, D.D.; Shen, Y.; Fang, Y.W.; Hu, L.J.; Liu, M.Y.; Dai, C.F.; Peng, S.L.; et al. Iron and magnetic: New research direction of the ferroptosis-based cancer therapy. *Am. J. Cancer Res.* **2018**, *8*, 1933–1946. [[PubMed](#)]
44. Watanabe, Y.; Nakagawa, M.; Miyakoshi, Y. Enhancement of lipid peroxidation in the liver of mice exposed to magnetic fields. *Ind. Health* **1997**, *35*, 285–290. [[CrossRef](#)] [[PubMed](#)]
45. Sabo, J.; Mirossay, L.; Horovcak, L.; Sarissky, M.; Mirossay, A.; Mojzis, J. Effects of static magnetic field on human leukemic cell line HL-60. *Bioelectrochemistry* **2002**, *56*, 227–231. [[CrossRef](#)]
46. Alvarez-Garcia, V.; Tawil, Y.; Wise, H.M.; Leslie, N.R. Mechanisms of PTEN loss in cancer: It's all about diversity. *Semin. Cancer Biol.* **2019**, *59*, 66–79. [[CrossRef](#)]
47. Cully, M.; You, H.; Levine, A.J.; Mak, T.W. Beyond PTEN mutations: The PI3K pathway as an integrator of multiple inputs during tumorigenesis. *Nat. Rev. Cancer* **2006**, *6*, 184–192. [[CrossRef](#)]
48. Tsutsui, S.; Inoue, H.; Yasuda, K.; Suzuki, K.; Higashi, H.; Era, S.; Mori, M. Reduced expression of PTEN protein and its prognostic implications in invasive ductal carcinoma of the breast. *Oncology* **2005**, *68*, 398–404. [[CrossRef](#)]
49. Ferraro, B.; Bepler, G.; Sharma, S.; Cantor, A.; Haura, E.B. EGR1 predicts PTEN and survival in patients with non-small-cell lung cancer. *J. Clin. Oncol.* **2005**, *23*, 1921–1926. [[CrossRef](#)]
50. Colakoglu, T.; Yildirim, S.; Kayaselcuk, F.; Nursal, T.Z.; Ezer, A.; Noyan, T.; Karakayali, H.; Haberal, M. Clinicopathological significance of PTEN loss and the phosphoinositide 3-kinase/Akt pathway in sporadic colorectal neoplasms: Is PTEN loss predictor of local recurrence? *Am. J. Surg.* **2008**, *195*, 719–725. [[CrossRef](#)]
51. Jang, K.S.; Song, Y.S.; Jang, S.H.; Min, K.W.; Na, W.; Jang, S.M.; Jun, Y.J.; Lee, K.H.; Choi, D.; Paik, S.S. Clinicopathological significance of nuclear PTEN expression in colorectal adenocarcinoma. *Histopathology* **2010**, *56*, 229–239. [[CrossRef](#)] [[PubMed](#)]
52. Sawai, H.; Yasuda, A.; Ochi, N.; Ma, J.; Matsuo, Y.; Wakasugi, T.; Takahashi, H.; Funahashi, H.; Sato, M.; Takeyama, H. Loss of PTEN expression is associated with colorectal cancer liver metastasis and poor patient survival. *BMC Gastroenterol.* **2008**, *8*, 56. [[CrossRef](#)] [[PubMed](#)]
53. Ahmad, I.; Morton, J.P.; Singh, L.B.; Radulescu, S.M.; Ridgway, R.A.; Patel, S.; Woodgett, J.; Winton, D.J.; Taketo, M.M.; Wu, X.R.; et al. beta-Catenin activation synergizes with PTEN loss to cause bladder cancer formation. *Oncogene* **2011**, *30*, 178–189. [[CrossRef](#)] [[PubMed](#)]
54. Lei, H.Q.; Furlong, P.J.; Ra, J.H.; Mullins, D.; Cantor, R.; Fraker, D.L.; Spitz, F.R. AKT activation and response to interferon-beta in human cancer cells. *Cancer Biol. Ther.* **2005**, *4*, 709–715. [[CrossRef](#)]
55. Huang, X.M.; Zhang, N.R.; Lin, X.T.; Zhu, C.Y.; Zou, Y.F.; Wu, X.J.; He, X.S.; He, X.W.; Wan, Y.L.; Lan, P. Antitumor immunity of low-dose cyclophosphamide: Changes in T cells and cytokines TGF-beta and IL-10 in mice with colon-cancer liver metastasis. *Gastroenterol. Rep. (Oxf.)* **2020**, *8*, 56–65. [[CrossRef](#)]
56. Rossowska, J.; Anger, N.; Szczygiel, A.; Mierzejewska, J.; Pajtasz-Piasecka, E. Reprogramming the murine colon cancer microenvironment using lentivectors encoding shRNA against IL-10 as a component of a potent DC-based chemoimmunotherapy. *J. Exp. Clin. Cancer Res.* **2018**, *37*, 126. [[CrossRef](#)]
57. Bhavsar, M.D.; Amiji, M.M. Oral IL-10 gene delivery in a microsphere-based formulation for local transfection and therapeutic efficacy in inflammatory bowel disease. *Gene Ther.* **2008**, *15*, 1200–1209. [[CrossRef](#)]
58. Apetoh, L.; Locher, C.; Ghiringhelli, F.; Kroemer, G.; Zitvogel, L. Harnessing dendritic cells in cancer. *Semin. Immunol.* **2011**, *23*, 42–49. [[CrossRef](#)]
59. Madhubala, V.; Pugazhendhi, A.; Thirunavukarasu, K. Cytotoxic and immunomodulatory effects of the low concentration of titanium dioxide nanoparticles (TiO₂ NPs) on human cell lines—An in vitro study. *Process Biochem.* **2019**, *86*, 186–195. [[CrossRef](#)]
60. Liu, J.Q.; Li, X.F.; Gu, C.Y.; da Silva, J.C.S.; Barros, A.L.; Alves, S.; Li, B.H.; Ren, F.; Batten, S.R.; Soares, T.A. A combined experimental and computational study of novel nanocage-based metal-organic frameworks for drug delivery. *Dalton Trans.* **2015**, *44*, 19370–19382. [[CrossRef](#)]

61. Li, F.M.; Li, B.H.; Wang, C.F.; Zeng, Y.P.; Liu, J.Q.; Gu, C.Y.; Lu, P.F.; Mei, L. Encapsulation of pharmaceutical ingredient linker in metal-organic framework: Combined experimental and theoretical insight into the drug delivery. *RSC Adv.* **2016**, *6*, 47959–47965. [[CrossRef](#)]
62. Qin, L.; Liang, F.L.; Li, Y.; Wu, J.A.; Guan, S.Y.; Wu, M.Y.; Xie, S.L.; Luo, M.S.; Ma, D.Y. A 2D Porous Zinc-Organic Framework Platform for Loading of 5-Fluorouracil. *Inorganics* **2022**, *10*, 202. [[CrossRef](#)]
63. Gurunathan, S.; Jeyaraj, M.; Kang, M.H.; Kim, J.H. Tangeretin-Assisted Platinum Nanoparticles Enhance the Apoptotic Properties of Doxorubicin: Combination Therapy for Osteosarcoma Treatment. *Nanomaterials* **2019**, *9*, 1089. [[CrossRef](#)]
64. Tran, N.; Webster, T.J. Understanding magnetic nanoparticle osteoblast receptor-mediated endocytosis using experiments and modeling. *Nanotechnology* **2013**, *24*, 185102. [[CrossRef](#)]

Disclaimer/Publisher's Note: The statements, opinions and data contained in all publications are solely those of the individual author(s) and contributor(s) and not of MDPI and/or the editor(s). MDPI and/or the editor(s) disclaim responsibility for any injury to people or property resulting from any ideas, methods, instructions or products referred to in the content.